

## Experimental investigation of equibiaxial extension and breakup of drops in a molten two-phase polymer blend

U. A. Handge

*Institute of Polymers, Department of Materials, ETH Zürich, Wolfgang-Pauli-Strasse 10, HCI H 529, 8093 Zürich, Switzerland*

(Received 1 December 2004; published 6 July 2005)

We experimentally investigate the breakup of an equibiaxially elongated polystyrene (PS) drop in a poly(methyl methacrylate) (PMMA) matrix during relaxation after melt elongation. In equibiaxial elongation, the initially spherical PS drop is deformed into an ellipsoidal disclike shape for our test parameters. Using a hotstage in combination with a light microscope, we observe the evolution of the drop shape during relaxation. In the initial stage of relaxation, fingers and holes are formed. The holes are located preferentially near the rim of the drop. The number and the size of the holes increase with time such that the elongated PS drop attains a complex shape during relaxation. The fingers form bulbous ends which separate from the fingers. We discuss the dynamics of this breakup process by taking into account the interfacial energy between PS and PMMA. Our analysis shows that a very large number of small PS droplets can be generated by the sequential breakup of the elongated PS drop.

DOI: [10.1103/PhysRevE.72.011801](https://doi.org/10.1103/PhysRevE.72.011801)

PACS number(s): 83.80.Tc, 47.20.Dr, 47.20.Ma

### I. INTRODUCTION

The deformation and breakup of drops in applied fields of flow at low Reynolds numbers are the subject of intensive theoretical and experimentally oriented research. Initiated by the work of Taylor [1], a series of investigations promoted understanding these phenomena. Different theoretical approaches were applied in order to model drop deformation [2–6], and the influence of the rheological properties of the drop and the matrix phase were the focus of experimental studies [7–9]. The progress in this field has been summarized in several review articles [10–13]. In the past, most studies were dedicated to the deformation of drops in shear flows or uniaxial and planar elongational flows, see, e.g., Refs. [14,15]. Only a few authors [16,17] theoretically investigated the deformation of drops in equibiaxial elongation and the possible breakup of equibiaxially extended drops. In the context of breakup phenomena, interfacial tension driven and free-surface flows such as the Rayleigh instability [18,19] have attracted much attention [20]. From a technological point of view, deformation and breakup phenomena strongly influence the development of the morphology of emulsions and blends of immiscible polymers [21] during mixing. Therefore these phenomena are technologically highly relevant, for example, in order to form well-controlled nearly monodisperse droplets [22,23].

In this study, we focus on relaxation phenomena in melts of polystyrene (PS)/poly(methyl methacrylate) (PMMA) blends which are caused by the interfacial tension [24–26]. We consider the deformation and relaxation of an initially spherical PS drop, which is embedded in a PMMA matrix after equibiaxial elongation in the molten state. If the spherical PS drop is elongated, the surface area of the drop increases. The surface area is proportional to the interfacial energy, and thus elastic energy is stored during elongation of the drop. When the applied flow is stopped, the drop minimizes its interfacial energy. For a large stretch ratio of the elongated drop, the interfacial energy of the elongated PS

drop exceeds the sum of the interfacial energies of several smaller drops whereby the total volume of these smaller drops equals the volume of the stretched PS drop. Consequently, such an elongated drop possibly does not retract back to a single spherical drop during relaxation, but breaks up into many smaller droplets.

We apply these considerations to the extension of a single drop which is surrounded by another fluid. First, we consider an arbitrary purely elongational flow. We denote the radius of the initially spherical drop by  $r_0$  and assume that drop and matrix phase are incompressible viscous fluids with shear viscosities  $\eta_d$  and  $\eta_m$ , respectively. In elongational flows, the velocity field  $\vec{v}=(v_x, v_y, v_z)$  far away from the drop is given by  $v_x=\dot{\epsilon}_0 x$ ,  $v_y=m\dot{\epsilon}_0 y$  and  $v_z=-(1+m)\dot{\epsilon}_0 z$ , where  $\dot{\epsilon}_0$  denotes the Hencky strain rate. The parameter  $m$  characterizes the type of flow and is  $m=-1/2$  in simple,  $m=0$  in planar, and  $m=1$  in equibiaxial elongation [27]. The ratio of the viscous stress of the matrix to the interfacial stress can be estimated by the capillary number  $\text{Ca}=\eta_m\dot{\epsilon}_0 r_0/\alpha$ , where  $\alpha$  denotes the interfacial tension between the two phases [3]. For a viscosity ratio  $p=\eta_d/\eta_m$  close to unity and a large capillary number  $\text{Ca}\gg 1$ , the drop is deformed into an approximately ellipsoidal shape during elongation [28]. We denote the principal axes of the extended drop parallel to the  $x$ ,  $y$ , and  $z$  directions by  $a$ ,  $b$ , and  $c$ , respectively. Since the volume  $V$  of the drop is conserved during elongation and  $V=4\pi abc/3$  holds, the principal axes  $a$ ,  $b$ , and  $c$ , of the elongated drop are given by  $a=r_0\lambda_d$ ,  $b=r_0\lambda_d^m$ , and  $c=r_0\lambda_d^{-(1+m)}$ . Here  $\lambda_d$  is the stretch ratio of the drop. Calculating the surface area of an ellipsoid of revolution [29], one finds that the surface area  $A$  of the elongated drop for  $\lambda_d\gg 1$  is given by  $A\approx(\pi r_0)^2\lambda_d^{1/2}$  in simple elongation and  $A\approx 2\pi r_0^2\lambda_d^2$  in equibiaxial elongation. These power laws reveal that the surface area of a long cylindrically shaped object generally is smaller than the surface area of a disclike object that both have the same volume. If the elongated drop breaks up into  $N$  smaller drops that finally retract to spheres with radius  $r$ , the surface area  $A_N$  of these smaller spheres is  $A_N=4N\pi r^2$ . The radius  $r$

TABLE I. Glass transition temperature  $T_g$ , density  $\rho$ , and zero shear viscosity  $\eta_0$  at 180°C of polystyrene PS 143 E and poly(methyl methacrylate) PMMA 5N.

	$T_g$ (°C)	$\rho$ at 180°C (g cm <sup>-3</sup> )	$\eta_0$ at 180°C (Pa s)
PS 143 E	85	0.98	$2.4 \times 10^4$
PMMA 5N	89	1.10	$3.2 \times 10^4$

of the spheres follows from the conservation of the volume which yields  $4N\pi r^3/3 = 4\pi r_0^3/3$  and thus  $r = r_0 N^{-1/3}$ . The elongated drop can only break up if the surface area  $A_N$  of the  $N$  spheres is smaller than the surface area  $A$  of the elongated drop. The condition  $A_N < A$  leads to  $N < (\pi/4)^3 \lambda_d^{3/2}$  in simple elongation and  $N < (1/8)\lambda_d^6$  in equibiaxial elongation. Therefore, we have  $N \geq 2$  for  $\lambda_d \geq 2.6$  in simple elongation and for  $\lambda_d \geq 1.6$  in equibiaxial elongation. Consequently, breakup is energetically possible. The equivalent number  $N_e$  of spheres with  $A_{N_e} = A$  for, e.g.,  $\lambda_d = 10$ , is  $N_e = (\pi/4)^3 \lambda_d^{3/2} = 15$  in simple elongation and  $N_e = (1/8)\lambda_d^6 = 125\,000$  in equibiaxial elongation which is a remarkable difference. In order to find out whether breakup of drops occurs after large deformations, we were thus motivated to observe experimentally the evolution of the drop shape during relaxation. In this work, we focus on relaxation after equibiaxial elongation which has also been the subject of theoretical studies [16,17].

## II. EXPERIMENTS

The polymers used in this study are blue-colored polystyrene PS 143 E of BASF AG, Ludwigshafen am Rhein, Germany (lot: 947 H 869, abbreviated by PS) and poly(methyl methacrylate) Plexiglas 5N of Degussa-Röhm, Darmstadt, Germany (lot: 425 953, abbreviated by PMMA). The glass transition temperature  $T_g$ , the density  $\rho$ , and the zero shear viscosity  $\eta_0$  of the homopolymers at 180°C are listed in Table I. The pellets were dried in vacuum at 65°C for at least 96 h. Then cylindrical samples of PS and PMMA for shear experiments were prepared by compression molding at 210°C during 240 min. The thickness of these samples was 1.5 mm and their diameter ranged between 14 mm and 20 mm.

We determined the complex modulus  $G^* = G' + iG''$  of PS and PMMA as a function of the angular frequency  $\omega$  at 180°C and 200°C in linear viscoelastic shear oscillations using a Physica UDS 200 (Physica, Stuttgart, Germany). A cone-and-plate geometry was used with a cone angle of 4° and the shear amplitude  $\gamma_0$  was set to  $\gamma_0 = 0.10$ . The data were shifted according to the time-temperature superposition principle to the reference temperature  $T_{\text{ref}} = 180^\circ\text{C}$  [30]. Then the zero shear viscosity  $\eta_0$  of PS and PMMA was obtained using the relation  $G''(\omega) = \eta_0 \omega$  for small  $\omega$ .

In order to observe the relaxation of a PS drop by light microscopy, we prepared samples for elongational rheometry in which a small number of PS drops (typically 5–20) were embedded into a PMMA matrix. First, PS filaments were spun at 220°C using a capillary rheometer Rheograph 2000 (Göttfert, Buchen/Odenwald, Germany). The die had a circu-

lar cross section with a diameter of 0.2 mm and a length of 1.0 mm. Then short pieces of the filaments were cut and placed between two PMMA plates with a thickness of 1 mm. This sandwich was compression molded at 210 °C during 240 min. Driven by the interfacial tension between PS and PMMA, the short PS fibres broke up and relaxed into a spherical shape during compression molding. The compression molded sheets were cut into samples for equibiaxial elongation experiments such that the PS drops were in the center of the sample. The thickness of the sample was 2 mm and the diameter of the reference area was 64 mm (see Ref. [27]).

We performed equibiaxial elongation experiments using the multiaxial elongational rheometer MAD (Multiaxiales Dehnrheometer) at 180 °C [27]. The sample was elongated with a Hencky strain rate of  $\dot{\epsilon}_0 = 0.1 \text{ s}^{-1}$  up to various values of the maximum Hencky strain  $\epsilon_{\text{max}}$ . For our test parameters, the elongated PS drop broke up during relaxation after elongation to  $\epsilon_{\text{max}} = 2.5$ . The value  $\epsilon_{\text{max}} = 2.5$  corresponds to the stretch ratio  $\lambda_{\text{max}} = \exp(2.5) = 12.2$ . Much smaller  $\epsilon_{\text{max}}$  values did not lead to the disintegration of the stretched PS drop. Larger  $\epsilon_{\text{max}}$  values required a very precise centering of the initial PS drop, because a decentered PS drop increased its distance to the center of the flow field exponentially with time and finally most probably left the reference area.

Immediately after the maximum Hencky strain had been attained at time  $t = 25 \text{ s}$ , we placed a sieve with cotton that was saturated by liquid nitrogen on top of the thin sample (thickness of the elongated sample  $\approx 13 \mu\text{m}$ ) in order to quench it. The solidified sample was cut at its rim and then carefully removed from the rheometer.

The elongated sample was placed between two PMMA plates with a thickness of 1 mm and a diameter of 15 mm. The purpose of this sandwich construction was to avoid boundary effects during relaxation. The sandwich was placed inside a silver ring onto a heating block in a hotstage (THMS 600, Linkam Scientific Instruments Ltd., Waterfield, UK) and heated up to 180 °C. We observed the relaxation of the drop with a light microscope (Optiphot-2, Nikon Corporation, Japan) that was connected to a digital camera (COOLPIX 995, Nikon Corporation, Japan).

## III. RESULTS

Figure 1 presents the results of our linear viscoelastic shear oscillations of PS and PMMA. Both materials behave like Newtonian fluids at low frequencies and thus for long relaxation times. The analysis of  $G''$  in the low frequency range yields  $\eta_0(\text{PS}) = 2.4 \times 10^4 \text{ Pa s}$  and  $\eta_0(\text{PMMA}) = 3.2 \times 10^4 \text{ Pa s}$ , which leads to a viscosity ratio  $p = \eta_0(\text{PS})/\eta_0(\text{PMMA}) = 0.75$ . In our equibiaxial elongation experiments, the spherical PS drop was deformed into a flat circular disc with stretch ratio  $\lambda_d$ . During relaxation, an elongated drop with a small stretch ratio retracted to a single drop which we observed for  $\lambda_d = 6.6$ . If the stretch ratio exceeded a certain limit, then breakup occurred. In the following, we describe the breakup scenario which we observed in our series of experiments.

The results of our microscopic investigations of the dynamics of the shape of the PS drop during subsequent relax-

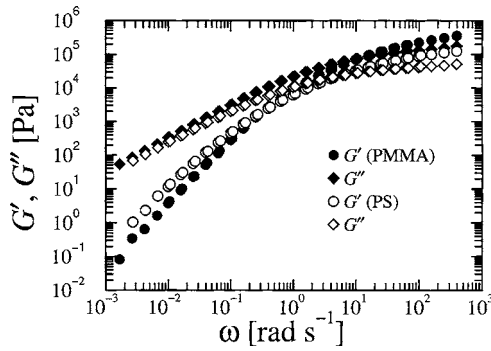


FIG. 1. Storage modulus  $G'$  and loss modulus  $G''$  as a function of  $\omega$  at  $T_{\text{ref}}=180^\circ\text{C}$  for PMMA 5N (filled symbols) and PS 143E (open symbols).

ation are presented in Fig. 2. For this experiment, the initial radius of the PS drop was  $r_0=35.5 \mu\text{m}$ . The capillary number was approximately  $\text{Ca}=\eta_0(\text{PMMA})\dot{\epsilon}_0 r_0/\alpha \approx 57$  where we used  $\alpha=2 \times 10^{-3} \text{ Nm}^{-1}$  [31,32]. After elongation of the

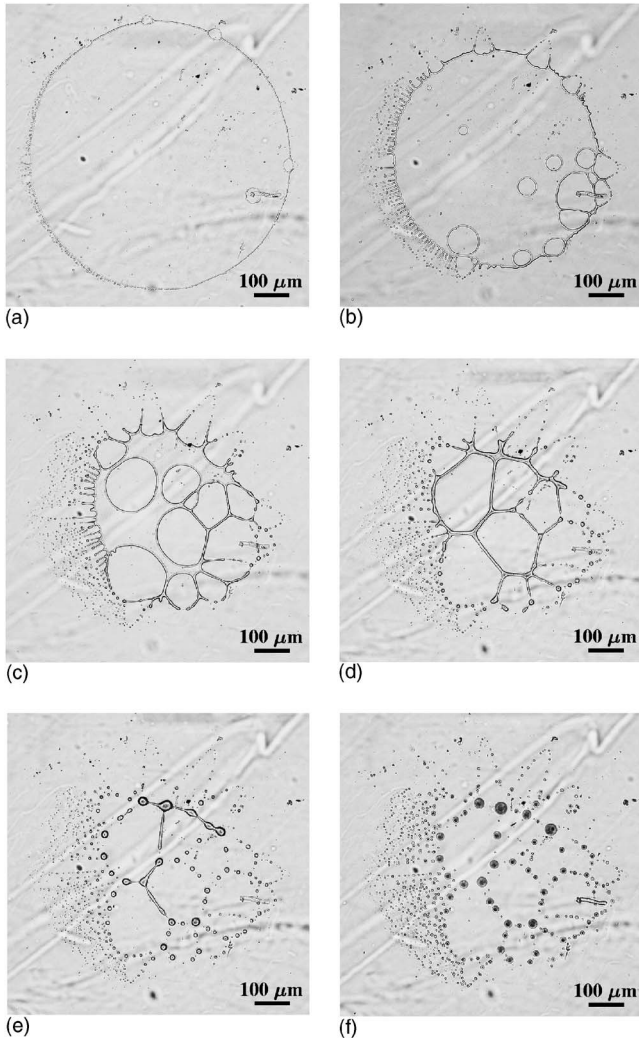


FIG. 2. Relaxation of an equibiaxially elongated PS drop. The time  $t'$  of relaxation is (a) 3 min, (b) 11 min, (c) 21 min, (d) 32 min, (e) 53 min, and (f) 84 min.

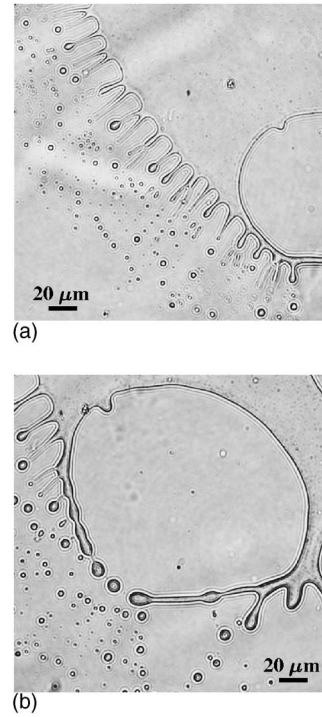


FIG. 3. Formation of fingers and holes. (a) Nearly equidistant fingers at the rim of the drop at relaxation time  $t'=13 \text{ min}$ . (b) Breakup of a bent PS filament at  $t'=19 \text{ min}$ .

sample to  $\epsilon_{\text{max}}=2.5$ , the radius  $r_d$  of the elongated drop was  $r_d=377 \mu\text{m}$ , which leads to the stretch ratio  $\lambda_d=r_d/r_0=10.6$ . For such large stretch ratios the disclike PS drop was very thin: The principal axis  $c$  of the elongated drop can be estimated by  $c=r_0\lambda_d^{-2}=0.31 \mu\text{m}$ . Figure 2(a) shows that holes were formed in the initial stage of relaxation. The holes were preferentially located near the rim of the circular disc and less frequently in the center of the drop; see Fig. 2(b). The size of these holes increased with time such that cylindrical PS filaments within the drop were formed when the rims of two neighbored holes approached each other. When the rim of a hole came close to the rim of the PS disc, a curved filament was formed. These fibril-like zones broke up into small spherical PS drops. In the initial stage, the number of the holes increased with time. At a later stage of relaxation, the formation of new holes terminated. Then the remaining drop had lost its ellipsoidal and attained a fibrillar shape [Figs. 2(c) and 2(d)]. This remaining part of the original PS drop relaxed and broke up into a small number of spheres. Finally the original PS drop was split up into a very large number of small drops, see Figs. 2(e) and 2(f).

Figure 3 shows a magnified view of a part of the rim of the PS drop during relaxation. In addition to the formation of holes, another relaxation process exists: Nearly equidistant fingers were formed at the left rim of the drop; see Fig. 3(a) and also Figs. 2(a) and 2(b). These PS fingers mainly occurred in the initial stage and formed bulbous ends which finally separated from the fingers. In our series of experiments, fingers were formed less frequently than holes. Figure 3(b) clearly reveals that a bent filament was formed near the rim of the drop with thicker and thinner zones which finally broke up into some PS drops.

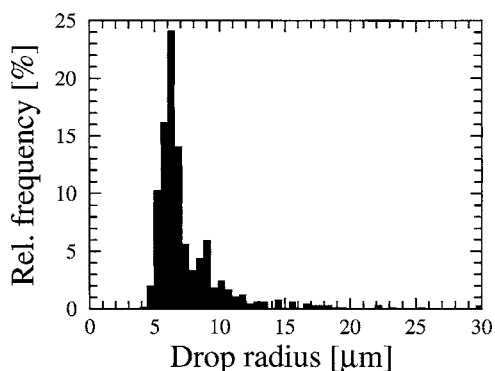


FIG. 4. Relative frequency of the radius of PS droplets at the end of the relaxation experiment of Fig. 2.

The remaining small PS drops created a pattern which was a fingerprint of the fragmentation process: The drops in the outer region had very small radii which resulted from the breakup of very thin filaments and fingers; see Fig. 2(f). In the center of the holes which were formed during relaxation, no drops were formed and hence these areas were empty. The drops in the center of the original PS drop were the largest ones and occurred in the later stages of our experiments. The number  $N$  of all PS droplets was approximately  $N=655$  and thus much smaller than the equivalent number of spheres  $N_e=(1/8)\lambda_d^6 \approx 177\,315$ . The large difference between  $N$  and  $N_e$  reveals that the dynamics of the breakup process strongly influences the final number of PS droplets. Figure 4 plots the relative frequency of the droplet radius. The distribution of the droplet radius is peaked at  $6\ \mu\text{m}$  which results from the large number of small droplets near the rim of the elongated PS disc. The relative frequency decreases for larger droplet radii. These radii belong to the small number of PS droplets which were formed near the center of the PS disc in the later stage of relaxation. At the end of the relaxation experiment, the radii of the PS droplets ranged between  $4$  and  $30\ \mu\text{m}$ . This interval is remarkably large and the droplet sizes are far away from being monodisperse.

The surface area of the PS drop increased tremendously during elongation. In subsequent relaxation, the interfacial energy was dissipated by the formation of holes and fingers. The locations where the holes appeared were randomly distributed. This observation gives a hint that deviations of the real drop shape from the ellipsoidal shape initiated the nucleation of holes. Such thickness variations can be caused by temperature inhomogeneities which lead to viscosity variations or by local variations of the value of the interfacial tension between PS and PMMA that are caused by tiny impurities. If a hole had been nucleated, then an increasing hole diameter drastically reduced the surface area of the PS disc and thus minimized the interfacial energy.

The formation of fingers also resulted from the minimization of the surface area. Generally, a cylinder has a smaller surface area than an ellipsoidal disc with the same volume which is evident from the power laws for the surface area  $A$  for a simply ( $A \propto \lambda_d^{1/2}$ ) and an equibiaxially elongated drop ( $A \propto \lambda_d^2$ ). Consequently, if a finger had been formed, then an increasing cylindrical finger decreased the surface area of the

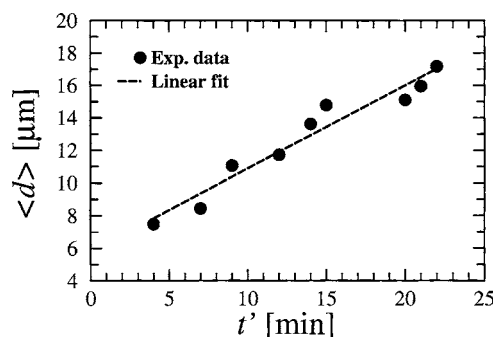


FIG. 5. Average distance  $\langle d \rangle$  between the fingers in the experiment of Fig. 2 as a function of relaxation time  $t'$ . The circles are the experimental data. The dashed line indicates a linear fit.

PS disc. In conclusion, the formation of fingers reduced the interfacial energy.

The fingers were nearly equidistantly distributed. The mean distance  $\langle d \rangle$  between two neighbored fingers increased approximately linearly with time, see Fig. 5, since with increasing time more and more fingers broke up into PS droplets and finally disappeared. At  $t'=31$  min almost all fingers had disappeared. This behavior indicates that the formation of fingers is influenced by the thickness of the PS disc. When the thickness of the retracting PS disc was too large, no more fingers were formed.

A breakup scenario which was similar to the one described here was observed in rupture and dewetting phenomena of thin PS films on a solid substrate [33–35]. In these experiments, holes were nucleated in the PS film. The diameter of the holes increased with time, which finally led to a polygon structure. The rims of the polygons were formed by the PS phase and finally disintegrated by the Rayleigh instability into small PS droplets. In addition, the fingering mechanism was also observed. In the experiments of Refs. [33,34], the PS films could be modelled by an infinite plane. On the contrary, in our experiments the elongated PS drop had a finite size and the thickness of the PS disc decreased towards its rim where the holes and the fingers were formed in the beginning of relaxation. Finally we remark that the formation of holes, which we observed here, resembles the formation of holes during the initial stage of blending of two immiscible polymers in the melt [36–39].

#### IV. SUMMARY

In summary, we observed the evolution of the shape of an equibiaxially elongated PS drop which was embedded in a PMMA matrix during relaxation in the molten state. A hot-stage in combination with a light microscope was used in order to observe the drop shape during relaxation. In equibiaxial elongation, the PS drop was deformed into a very flat circular disc for our test parameters. During relaxation, holes and fingers were formed. The holes were formed near the rim of the PS disc and increased in number and in size with time. The fingers formed a bulbous end that separated from the fingers. At the later stage of relaxation, the original PS drop attained a fibrillar shape and finally was disintegrated into a

large number of small droplets. Our analysis revealed that the formation of holes and fingers was both associated with a minimization of the interfacial energy. Since the interfacial area increases much more during equibiaxial elongation than during uniaxial elongation, the interfacial tension driven breakup of an equibiaxially elongated drop can lead to a much larger number of small droplets than the breakup of a uniaxially stretched drop.

#### ACKNOWLEDGMENTS

The author is very thankful to Professor J. Meissner and Professor H.C. Öttinger for valuable and stimulating discussions that contributed very much to this work. He is indebted to F. Eckermann, J. Hostettler, F. Mettler, W. Schmidheiny, and P. Zihlmann for their support and to M. Colussi for the DSC measurements.

- 
- [1] G. I. Taylor, Proc. R. Soc. London, Ser. A **146**, 501 (1934).  
 [2] D. Barthès-Biesel and A. Acrivos, J. Fluid Mech. **61**, 1 (1973).  
 [3] A. Acrivos and T. S. Lo, J. Fluid Mech. **86**, 641 (1978).  
 [4] P. L. Maffettone and M. Minale, J. Non-Newtonian Fluid Mech. **78**, 227 (1998).  
 [5] B. J. Edwards and M. Dressler, Rheol. Acta **42**, 326 (2003).  
 [6] W. Yu and M. Bousmina, J. Rheol. **47**, 1011 (2003).  
 [7] H. A. Stone, B. J. Bentley, and L. G. Leal, J. Fluid Mech. **173**, 131 (1986).  
 [8] F. Mighri, A. Ajji, and P. J. Carreau, J. Rheol. **41**, 1183 (1997).  
 [9] S. Guido and M. Villone, J. Rheol. **42**, 395 (1998).  
 [10] H. P. Grace, Chem. Eng. Commun. **14**, 225 (1982).  
 [11] J. M. Rallison, Annu. Rev. Fluid Mech. **16**, 45 (1984).  
 [12] H. A. Stone, Annu. Rev. Fluid Mech. **26**, 65 (1994).  
 [13] C. L. Tucker III and P. Moldenaers, Annu. Rev. Fluid Mech. **34**, 177 (2002).  
 [14] S. Ramaswamy and L. G. Leal, J. Non-Newtonian Fluid Mech. **88**, 149 (1999).  
 [15] D. C. Tretheway and L. G. Leal, J. Non-Newtonian Fluid Mech. **99**, 81 (2001).  
 [16] H. A. Stone and L. G. Leal, J. Colloid Interface Sci. **133**, 340 (1989).  
 [17] I. S. Kang and L. G. Leal, Phys. Fluids A **1**, 644 (1989).  
 [18] Lord Rayleigh, Proc. London Math. Soc. **10**, 4 (1878).  
 [19] S. Tomotika, Proc. R. Soc. London, Ser. A **150**, 322 (1935).  
 [20] J. Eggers, Rev. Mod. Phys. **69**, 865 (1997).  
 [21] D. R. Link, S. L. Anna, D. A. Weitz, and H. A. Stone, Phys. Rev. Lett. **92**, 054503 (2004).  
 [22] C. Cramer, B. Berüter, P. Fischer, and E. J. Windhab, Chem. Eng. Technol. **25**, 499 (2002).  
 [23] K. Feigl, S. F. M. Kaufmann, P. Fischer, and E. J. Windhab, Chem. Eng. Sci. **58**, 2351 (2003).  
 [24] E. van Hemelrijck, P. van Puyvelde, and P. Moldenaers, Langmuir **20**, 3498 (2004).  
 [25] H. A. Stone and L. G. Leal, J. Fluid Mech. **198**, 399 (1989).  
 [26] M. Tjahjadi, H. A. Stone, and J. M. Ottino, J. Fluid Mech. **243**, 297 (1992).  
 [27] P. Hachmann and J. Meissner, J. Rheol. **47**, 989 (2003).  
 [28] I. Delaby, B. Ernst, Y. Germain, and R. Muller, J. Rheol. **38**, 1705 (1994).  
 [29] W. I. Smirnow, *Lehrgang der höheren Mathematik Teil I*, 16th ed. (Verlag Harri Deutsch, Berlin, 1990), pp 243.  
 [30] J. Honerkamp and J. Weese, Rheol. Acta **32**, 57 (1993).  
 [31] H. Gramespacher and J. Meissner, J. Rheol. **41**, 27 (1997).  
 [32] U. A. Handge, J. Rheol. **48**, 1103 (2004).  
 [33] G. Reiter, Phys. Rev. Lett. **68**, 75 (1992).  
 [34] G. Reiter, Langmuir **9**, 1344 (1993).  
 [35] S. Herminghaus, A. Fery, S. Schlagowski, K. Jacobs, R. Seemann, H. Gau, W. Mönch, and T. Pompe, J. Phys.: Condens. Matter **12**, A57 (2000).  
 [36] U. Sundararaj, Y. Dori, and C. W. Macosko, Polymer **36**, 1957 (1995).  
 [37] C. E. Scott and C. W. Macosko, Polymer **36**, 461 (1995).  
 [38] D. A. Zumbrunnen and C. Chhibber, Polymer **43**, 3267 (2002).  
 [39] D. A. Zumbrunnen, S. Inamdar, O. Kwon, and P. Verma, Nano Lett. **2**, 1143 (2002).